SPATIAL FREQUENCY RESPONSE OF AN

OPTICAL HETERODYNE RECEIVER

Carl L. Fales and Don M. Robinson
Langley Research Center

SUMMARY

The principles of transfer function analysis have been applied to a
passive optical heterodyne receiver to obtain the modulation transfer function
(MTF). MTF calculations have been performed based of an optical platform
which is imaging vertically varying profiles at worst case shuttle orbit
altitudes. An analysis of the derogatory effects of sampling (aliasing) and
central obscurations on both resolution and heterodyne efficiency is given.

INTRODUCTION

One measure of performance of an optical imaging system is its ability to
reproduce an object distribution with sufficient signal-to-noise ratio and
resolution so as to make the information contained within the image useful.
Generally, such a system may be characterized by its optical transfer function
(OTF) or, in certain cases, by the modulation transfer function (MTF) (ref. 1).

For conventional imaging systems using either coherent or incoherent
illumination, one usually assumes linearity in the imaging process so that the
cascading property of transfer function analysis applies (ref. 2). Under this
assumption, the MTF's of the individual subsystems (i.e., optics, detector,
electronics, etc.) can be multiplied to give the overall transfer function.

In this paper, the principles of transfer function analysis have been
applied to a passive optical heterodyne receiver which is assumed to be
imaging vertically varying spatial profiles at worst-case shuttle orbit
altitudes. Results of the analysis show some interesting departures from the
properties described above; namely, that the cascading property must be
carefully applied and that optical receivers having obscurations, such as a
Cassegrains, are not optimum for heterodyne-type detection.

THEORETICAL ANALYSIS

Imaging Considerations

Consider an optical receiver which is imaging an object amplitude
distribution as shown in figure 1. Using scalar diffraction theory, the signal
amplitude, E_s, in the detector plane, $\underline{r}$, is given by (ref. 3)

$$E_s(\underline{r}) = E_g(\underline{r}) \, \circledast \, h(\underline{r}) = \int_{-\infty}^{+\infty} d^2s \, E_g(\underline{s}) h(\underline{r} - \underline{s}) \qquad (1)$$

where $h(\underline{r})$ is the impulse response of the imaging optics and $E_g(\underline{r})$ is the amplitude of the geometrical image of the object. The shift invariance of $h(\underline{r})$ can be justified for the heterodyne applications discussed here by a careful examination of the various phase factors appearing in the impulse response function.

For mixing of two deterministic optical beams in an ideal detector, the mean-square heterodyne current power at the difference frequency, $f = |\nu - \nu_o|$ is (ref. 4)

$$I_{het}^2 = \frac{2\eta^2 e^2}{(h\nu)^2} \left| \int_{det} d^2r \, E_o^*(\underline{r}) \, E_s(\underline{r}) \right|^2 \qquad (2)$$

where $E_o(\underline{r})$ is the local oscillator amplitude distribution in the detector plane, η is the quantum efficiency, e is the electronic charge, and $h\nu$ is the photon energy. A simple-minded classical approach is taken to obtain the correct expression from which the spatial frequency analysis may begin. We recognize that the geometrical image field, $E_g(s,\nu)$, is a stochastic process which we synthesize by discrete frequency components with random phases. Now, for a deterministic L.O. field and a quasi-monochromatic optical signal, equation (1) and the generalization of equation (2) combine to give

$$I_{het}^2 = \frac{2\eta^2 e^2}{(h\nu)^2} \sum_f \int\!\!\int_{-\infty}^{+\infty} d^2s \, d^2s' \, <E_g(\underline{s},f+\nu_o)E_g^*(\underline{s}',f+\nu_o)> \left[\int_{det} dr^2 E_o^*(\underline{r}) h(\underline{r}-\underline{s}) \right]$$

$$\left[\int_{det} d^2r' E_o(\underline{r}') h^*(r'-s') \right] \qquad (3)$$

where $< \, >$ represents an average over the ensemble of signal fields. It is assumed that the source, i.e., the sun, of the image field on the detector is spatially incoherent. The appropriate substitutions are

$$<E_g(\underline{s}, \nu) E_g^*(\underline{s}', \nu)> \rightarrow \Delta f \, \lambda^2 P_g(\underline{s}, \nu) \delta(\underline{s} - \underline{s}')$$

$$I_{het}^2 \rightarrow I_{het}^2(f)\Delta f$$

where P_g represents the image spectral radiance at the detector plane in $W/m^2/str/Hz$ and $I_{het}^2(f)$ is the current spectral power density in A^2/Hz.

Equation (3) becomes

$$I_{het}^2(f) = \frac{2\eta^2 e^2 \lambda^2}{(h\nu)^2} \int_{-\infty}^{+\infty} d^2s [P_g(\underline{s}, \nu_o + f) + P_g(\underline{s}, \nu_o - f)] |T_o^*(\underline{s}) \otimes h(-\underline{s})|^2$$

where $f \geq 0$ and we note that the L.O. mixes with the signal field components at $\nu_o + f$ and $\nu_o - f$. Here, we have expressed the detector overlap integral of the L.O. field and the impulse response function as

$$\int_{-\infty}^{+\infty} T_{det}(\underline{r}) E_o^*(\underline{r}) h(\underline{r} - \underline{s}) d^2r = T_o^*(\underline{s}) \otimes h(-\underline{s})$$

where $T_{det}(\underline{r})$ is the aperture function of the detector geometry and the product $T_{det}(\underline{r}) E_o^*(\underline{r}) = T_o^*(\underline{r})$ is simply that portion of the L.O. that is transmitted by the detector aperture.

Referring to the detector scheme of figure 2, the output current from the synchronous detector is

$$I_{sync} = \frac{2Te^2\eta^2\lambda^2}{(h\nu)^2} \int_{-\infty}^{+\infty} d^2s \int_{(f>0)} df |H_{het}(f)|^2 [P_g(\underline{s},\nu_o+f) + P_g(\underline{s},\nu_o-f)]|T_o^*(\underline{s})$$

$$\otimes h(-\underline{s})|^2$$

where H_{het} is the total heterodyne transfer function defined by

$$|H_{het}(f)|^2 = |H_m|^2 |H_d|^2 |H_{ifa}|^2$$

and T is the optical transmission factor. The various contributions to H_{het} are (1) the signal/L.O. mixing transfer function, H_m, representing carrier diffusion and transit time effects in the detector; (2) the photo-detector transfer function, H_d, comprised of contributions due to capacitance, resistance and inductance; and (3) the I.F. amplifier and filter transfer function, H_{ifa}. The square-law detector is assumed to have a unity transfer function ($H_{sq} = 1$). The shot noise transfer function, H_{tr}, is due only to transit time effects as opposed to H_m.

Heterodyne Transfer Function

In this paper, we are interested in the spatial frequency response of the heterodyne receiver to a vertically varying object profile as shown in figure 1. This is different from the I.F. considerations discussed previously other than a knowledge of the total I.F. power. To obtain the spatial frequency response and, ultimately, the system modulation transfer function (MTF), we assume the object scene radiance (and, consequently, the image scene) is linearly translated due to motion of the optical receiver, e.g., an orbiting platform. This induces a translation of the image coordinates by an amount

$$\underline{s} \rightarrow \underline{s} - \underline{r}(t)$$

and

$$P_g(\underline{s}, \nu_o \pm f) \rightarrow P_g(\underline{s} - \underline{r}, \nu_o \pm f)$$

Further, we define

$$P_g(-\underline{r}) \equiv \int\limits_{(f>0)} df |H_{het}(f)|^2 [P_g(\underline{r}, \nu_o + f) + P_g(\underline{r}, \nu_o - f)]$$

Since the impulse response, h, is invariant, we have the output current from the synchronous detector as

$$I_{sync}(t) = I_{sync}[\underline{r}(t)] = \frac{2Te^2\eta^2\lambda^2}{(h\nu)^2} \int\limits_{-\infty}^{+\infty} d^2s \, P_g(\underline{r} - \underline{s}) |T_o^*(\underline{s}) \, \circledast \, h(-\underline{s})|^2 \qquad (4)$$

Equation (4) is of the form of a convolution

$$I_{sync}[r(t)] = \frac{2Te^2\eta^2\lambda^2}{(h\nu)^2} P_g(\underline{r}) \, \circledast \, |T_o^*(\underline{r}) \, \circledast \, h(-\underline{r})|^2$$

Decomposition of I_{sync} into its spatial frequency components is obtained by the Fourier transformation

$$\hat{I}_{sync}(\underline{K}) = \int\limits_{-\infty}^{\infty} e^{-i2\pi\underline{K}\cdot\underline{r}} I_{sync}(\underline{r}) d^2r$$

Using the convolution theorem, we have

$$\hat{I}_{sync}(\underline{K}) = \frac{2Te^2\eta^2\lambda^2}{(h\nu)^2} G_g(\underline{K}) [G_o^*(-\underline{K})H(-\underline{K}) \otimes G_o(\underline{K})H^*(\underline{K})] \tag{5}$$

where $\underline{K}$ is the spatial frequency vector variable defined by its rectangular components (K_x, K_y), $G_g(\underline{K})$ is the object, or more specifically, the geometrical image spectrum, $G_o(\underline{K})$ is the detector pupil function modulated L.O. spectrum, and $H(\underline{K})$ is the coherent transfer function of the system (ref. 3).

Equation (5) illustrates the departure of the transfer function obtained in a heterodyne system with that obtained in conventional imaging systems. Remembering that the coherent transfer function, $H(\underline{K})$, is equal to the pupil function of the optical receiver (with a suitable change in variables) (ref. 3), the conventional optical transfer function is proportional to

$$G_{det}(\underline{K}) [H(-\underline{K}) \otimes H^*(\underline{K})]$$

where $G_{det}(\underline{K})$ is the Fourier transform of the detector aperture function, $T_{det}(\underline{K})$. In equation (5), however, we see that $H(\underline{K})$ is modified by the spectrum of the L.O./detector combination, $G_o(K)$. The normalized convolution of the product $G_o(\underline{K})H^*(\underline{K})$ with its negative argument complex conjugate is defined as the heterodyne transfer function, G_H. Functionally, then, we define a normalized heterodyne transfer function by

$$G_H(\underline{K}) \equiv \frac{G_o^*(-\underline{K})H(-\underline{K}) \otimes G_o(\underline{K})H^*(\underline{K})}{[G_o^*(-\underline{K})H(-\underline{K}) \otimes G_o(\underline{K})H^*(\underline{K})]_{\underline{K}=0}} \tag{6}$$

or

$$G_H(\underline{K}) = \frac{\int d^2K' G_o(\underline{K}')H^*(\underline{K}')G_o^*(\underline{K}'-\underline{K})H(\underline{K}'-\underline{K})}{\int d^2K' |G_o(\underline{K}')|^2 |H(\underline{K}')|^2}$$

Heterodyne Efficiency Factor

The denominator of equation (6) indicates that the product $G_o(\underline{K})H(\underline{K})$ represents the optics/L.O. detector amplitude spectrum that is transferred to the detector. Using Parseval's theorem, the integral $\int d^2K |G_o(\underline{K})|^2 |H(\underline{K})|^2$ is thus the power available for heterodyning out of a total L.O.-detector power of $P_o = \int d^2K |G_o(\underline{K})|^2$. For a uniform extended source, we may thus define an efficiency factor

$$\chi \equiv \frac{\int d^2 K \, |G_0(\underline{K})|^2 |H(\underline{K})|^2}{\int d^2 K \, |G_0(\underline{K})|^2} \le 1 \tag{7}$$

With this definition, the current spectrum for the synchronous detector (equation (5)) becomes

$$\hat{I}_{sync}(\underline{K}) = \frac{2Te^2\eta^2\lambda^2}{(h\nu)^2} P_0 \chi G_H(\underline{K}) G_g(\underline{K}) \tag{8}$$

Equation (8) may be related to a more conventional form of heterodyne efficiency found in the literature (ref. 5). The synchronous detector current is the inverse Fourier transform of equation (8), i.e.,

$$I_{sync}(\underline{r}) = \int_{-\infty}^{+\infty} d^2K \, \hat{I}_{sync}(\underline{K}) \, e^{i2\pi\underline{K}\cdot\underline{r}}$$

For a stationary scene, i.e., before translation of the image coordinates, we have $\underline{r} = 0$ so that

$$I_{sync}(0) = \int_{-\infty}^{+\infty} \hat{I}_{sync}(\underline{K}) \, d^2K \tag{9}$$

Substitution of equation (8) into equation (9) and assuming a blackbody source of geometrical shape factor, $A_g(\underline{r})$, and radiance $P_g(\underline{r})$, we have

$$P_g(\underline{r}) = \frac{2h\nu \, B_{HIF}}{\lambda^2(e^{h\nu/KT} - 1)} \, A_g(\underline{r})$$

and

$$I_{sync}(\underline{r} = 0) = \frac{4Te^2\eta^2 P_0 B_{HIF}}{h\nu(e^{h\nu/KT} - 1)} \chi \int_{-\infty}^{+\infty} d^2K \, \hat{A}_g(\underline{K}) G_H(\underline{K}) \tag{10}$$

where mixing occurs over an effective bandwidth $2B_{HIF}$ centered at the L.O. frequency, a polarization loss factor of 0.5 is included, and $\hat{A}_g(\underline{K})$ is the Fourier transform of $A_g(\underline{r})$. The integral portion of equation (10) has the form of a throughput, i.e., that portion of the image passed by the heterodyne

500

transfer function. The product of χ and this integral is an efficiency

$$\chi_{het} \equiv \chi \int_{-\infty}^{+\infty} d^2K \; \hat{A}_g(\underline{K}) \, G_H(\underline{K}) \tag{11}$$

so that equation (10) becomes

$$I_{sync}(r = 0) = \frac{4Te^2 \eta^2 P_o B_{HIF} \chi_{het}}{h\nu(e^{h\nu/KT} - 1)}$$

If now, we define a shot noise level due to the L.O. by

$$N = \frac{2\eta e^2}{(h\nu)} P_o B_{SIF}$$

then the signal-to-noise ratio in the shot noise limit becomes

$$\frac{S}{N} = \frac{I_{sync}(r = 0)}{N} = \frac{2T}{(e^{h\nu/KT} - 1)} \eta_{het} \cdot \frac{B_{HIF}}{B_{SIF}}$$

where we have defined

$$\eta_{het} \equiv \eta \, \chi_{het} \leq \eta$$

as the heterodyne quantum efficiency and B_{SIF} is the effective shot noise bandwidth. Note that for a uniform extended source, $A_g(\underline{K}) = \delta(\underline{K})$ and equation (11) reduces to $\chi_{het} = \chi$ and $\eta_{het} = \eta\chi$. In this case, the efficiency factor, χ, which we have defined in equation (7) is equivalent (to within the D.C. quantum efficiency, η) to the heterodyne quantum efficiency, η_{het}, found in the literature (ref. 5).

System Transfer Function

Results from the previous section may now be used to calculate the system transfer function, including the low-pass filter (see figure 2), for the specific case of imaging a one-dimensional object through an optical receiver which has rectangular symmetry. This case has some physical significance since the resolution elements of interest in an orbiting heterodyne receiver are vertically varying stratospheric layers. In addition, to avoid scaling difficulties in the calculations we will use angular coordinates defined by (see figure 1)

$$\theta = \frac{X}{d_i} \quad ; \quad \phi = \frac{Y}{d_i} \quad \text{(radians)}$$

$$K_\theta = K_X d_i \quad ; \quad K_\phi = K_Y d_i \quad \text{(cycles/radian)} \tag{12}$$

and

$$\theta_F = \frac{\ell_X}{d_i} \quad \text{(radians)}$$

where θ_F is the geometrical instantaneous field of view (I.F.O.V.) of the optical receiver.

Using equations (12) and the one-dimensional geometry, equation (6) becomes

$$G_H(K_\theta; K_C, \theta_F) = \frac{[\text{sinc}(\theta_F K_\theta)\,\text{RECT}(\frac{K_\theta}{2K_C})] \circledast [\text{sinc}(\theta_F K_\theta)\,\text{RECT}(\frac{K_\theta}{2K_C})]}{\{[\text{sinc}(\theta_F K_\theta)\,\text{RECT}(\frac{K_\theta}{2K_C})] \circledast [\text{sinc}(\theta_F K_\theta)\,\text{RECT}(\frac{K_\theta}{2K_C})]\}_{K_\theta=0}} \tag{13}$$

where

$$\text{sinc}(X) \equiv \frac{\sin \pi X}{\pi X} \quad \text{and} \quad \text{RECT}(\frac{X}{2\ell}) \equiv \begin{cases} 1 \,, & |X| \le \ell \\ 0 \,, & |X| > \ell \end{cases}$$

Equation (13) assumes a plane wave local oscillator incident of the detector so that the detector/L.O. transfer function becomes simply the Fourier transform of the detector aperture. Further, the coherent transfer function for the optics is the pupil function (rectangular in shape) having a coherent cut-off frequency of $K_C = D_A/2\lambda$, where D_A is the diameter of the receiver aperture and λ the wavelength. This convolution process is shown in figure 3.

Equation (13) along with equation (8) gives the system transfer function up to the low-pass filter. Expressing $G_H(K_\theta; K_C, \theta_F)$ and $\chi(K_C, \theta_F)$ (equation (7)) in integral form, we have

$$G_H(K_\theta; K_C, \theta_F) = \frac{\displaystyle\int_{-\infty}^{+\infty} \text{sinc}(\theta_F K_\theta')\,\text{RECT}(\frac{K_\theta'}{2K_C})\,\text{sinc}[\theta_P(K_\theta'-K_\theta)]\,\text{RECT}(\frac{K_\theta'-K_\theta}{2K_C})\,dK_o'}{\displaystyle\int_{-\infty}^{+\infty} \text{sinc}^2(\theta_F K_\theta)\,\text{RECT}(\frac{K_\theta}{2K_C})\,dK_o}$$

$$\tag{14}$$

and

$$\chi(K_\theta, \theta_P) = \theta_P^2 \left[\int_{-\infty}^{+\infty} \text{sinc}^2(\theta_F K_\theta) \, \text{RECT}(\frac{K_\theta}{2K_c}) \, dK_\theta \right]^2 \tag{15}$$

Finally, inclusion of the low-pass filter transfer function, H_{LP}, (i.e., the integration time, τ) which, in this case is modeled as a running mean integrator, we have

$$H_{LP}(K_\theta) = \text{sinc}(\frac{v_o \tau}{z} K_\theta)$$

where v_o is the vertical component of the orbital velocity, z the receiver-object distance, and τ the integration time. The total transfer function is then the modulation transfer function

$$MTF(K_\theta) = \left| G_H(K_\theta) H_{LP}(K_\theta) \right|$$

Equations (14) and (15) can be evaluated in terms of tabulated functions yielding the following relations which will be used for computational purposes

$$MTF(K_\theta; \theta_F, K_c, \frac{v_o \tau}{z}) = (N) \, \text{RECT}(\frac{K_\theta}{4K_c}) \left| \text{sinc}(\frac{v_o \tau}{z} K_\theta) \left\{ \left(\frac{\cos(\pi \theta_F K_\theta)}{\pi \theta_F K_\theta} \right) X \right. \right.$$

$$[C_{in}(|2\pi \theta_F K_\theta - 2\pi \theta_F K_c|) - C_{in}(2\pi \theta_F K_c)] +$$

$$\left. \left. \left(\frac{\sin(\pi \theta_F K_\theta)}{\pi \theta_F K_\theta} \right) [s_i(2\pi \theta_F K_c| - s_i(2\pi \theta_F K_\theta - 2\pi \theta_F K_c)] \right\} \right| \tag{16}$$

$$\chi(\theta_F, K_c) = \frac{4}{\pi^2} [s_i(2\pi \theta_F K_c) - \frac{1 - \cos(2\pi \theta_F K_c)}{2\pi \theta_F K_c}]^2 \quad \text{and} \quad N = (\pi \chi^{1/2})^{-1}$$

In the above equations, the functions $C_{in}(X)$ and $s_i(X)$ are defined as (ref. 6)

$$s_i(X) = \int_0^X \frac{\sin t}{t} \, dt \quad \text{and} \quad C_{in}(X) = \int_0^X \frac{1 - \cos t}{t} \, dt$$

RESULTS AND DISCUSSION

MTF Calculations

Equations (16) and (17) may now be evaluated for some specific parameter values which are applicable to the optical receiver in a space-lab type of scenario. A worst-case set of orbital values would be for the receiver platform to be at an orbital height of $R = 400$ Km and a tangent height, H_T, of 10 Km. At these values, we assume that the receiver is operating in a solar occultation mode where the sunrise or sunset velocity due to orbital motion is $v_o = 2$ Km/sec. The MTF and χ calculations (equations (16) and (17)) will be done for an I.F.O.V. of $\theta_F = 0.5 \times 10^{-3}$ rad , an equivalent optical receiver aperture of $D_A = 2.0"$, and values of integration time of $\tau = 0.2$ sec , and 0.4 sec. Further, the value of $D_A = 2.0"$ at a wavelength of $\lambda = 11.152$ µm (HNO_3 line) corresponds to an optics cut-off frequency of $K_c = D_A/2\lambda = 2278$ cycles/radian. These parameters are compatible with the values for an LHS type experiment using a tunable diode laser as the L.O. and associated optics for coupling this type radiation to a detector having the required time-frequency response (ref. 7).

The calculations are shown in figure 4. It can be shown that, for values of τ greater than roughly 0.2 sec., the optical (heterodyne) transfer function dominates the MTF; and, for τ somewhat less than 0.4 sec., the low pass filter is the dominant frequency limiting factor. Note that the angular frequency values can be converted to linear spatial frequency (cycles/Km) by the relationships of equation (12) by appropriately scaling image and object space by the ratio of image distance, d_i, to object distance, z. For the orbital values assumed, $z = 2262$ Km and consequently a value of 2262 cycles/rad corresponds to an object spatial frequency of 1 cycle/Km. Examination of the MTF curves shows that resolutions of the order of 1.5-2.0 Km may be expected for the various integration times.

Efficiency Calculations

The efficiency factor (heterodyne efficiency) given by equation (17) is shown plotted in figure 5 for the case of the plane-wave L.O.. Two geometries are shown: rectangular optics (as has been previously assumed) and circular optics adjusted for equal optics and detector areas. The significance of the abscissa ($2\pi\theta_F K_c$) relative to heterodyne efficiency becomes apparent when it is noted that at the value of $2\pi\theta_F K_c \cong 7.7$ corresponds approximately to an image (sun) size filling the detector of one Airy Disk of the receiver aperture. In this region, the efficiency is in excess of 80%.

Sampling Error

The calculations shown plotted in figure 5 do not include any sampling errors which may occur. Suppose we sample the output of the low-pass filter, which has been modeled as a running mean integrator, at a rate of the inverse of the integration time. This is equivalent to a sampled mean integration scheme. Under this constraint, it may be shown that for certain values of τ the signal is undersampled. This results in an aliasing or foldover error which can be significant relative to the desired signal. For example, shown in figure 6 is the total MTF for the values of orbital and system parameters previously stated. Two integration times are considered: $\tau = 0.2$ sec and $\tau = 0.4$ sec. If we define the sampling error as the ratio of the "foldover" amplitude on the MTF plot to the amplitude of the MTF itself, i.e., a white signal spectrum, we see that the error for 0.4 sec. is approximately 40% at 0.5 cycle/Km frequency and considerably worse for higher values of spatial frequency. Conversely, for $\tau = 0.2$ sec and the correspondingly higher sampling rate, the sampling error is negligible.

Heterodyne Receivers With Obscurations

Telescopes having central obscurations such as Cassegrains are often used for imaging a source. If this type receiver is used as a collector for heterodyne-type detection, one needs to compare the efficiency, χ, and the heterodyne transfer function, G_H, with that obtained for the unobscured case.

In figure 7, we consider the effects of receiver apertures having obscuration ratios of 0 and 20% for $\theta_F = 0.2 \times 10^{-3}$ and 0.5×10^{-3} rad. Note the enhancement of response in the 2000 cycles/rad region at the expense of that near 1000 cycles/rad for 20% obscuration and $\theta_F = 0.5 \times 10^{-3}$ rad. The effects of obscurations are more pronounced for square as opposed to circular geometries. An unobscured conventional MTF discussed earlier is plotted for $\theta_F = 0.5 \times 10^{-3}$ rad showing a somewhat reduced frequency response characteristic from the heterodyne MTF. For a smaller detector ($\theta_F = 0.2 \times 10^{-3}$ rad), a 20% obscuration tends to assume the shape of a conventional MTF.

In figure 5, we assume a receiver aperture having obscuration ratios of 20% and 50%. For the values of θ_F and K_c used earlier, $X = 2\pi\theta_F K_c \cong 7.2$, and comparison of the various efficiency curves at this value shows striking differences. For the 50% case, one sees that the heterodyne efficiency is virtually zero while for the 20% case a relative efficiency of slightly greater than 0.2 is achieved. This compares with a value of greater than 0.8 in the unobscured case. Note further there is a "peaking" of the efficiency curves for obscured systems. The rule-of-thumb requirement of one Airy disk on the detector for "good" efficiency no longer holds but rather the source image needs to be less than this value to achieve the maximum efficiency for that particular system. The effect can be explained on the basis of the overlap integral (equation (2)) of the L.O. field and signal field

distributions. Thus, the diffracted field due to the central obscuration is out of phase with that of the primary diffracted field and, as the size of the detector and/or optics increases, the cancellation tends to be more complete.

CONCLUDING REMARKS

The analysis of a passive heterodyne receiver with respect to its imaging performance (transfer function) and its heterodyne efficiency shows some interesting departures from the results which are obtained in strictly coherent or incoherent imaging systems. For example, the cascading property of MTF analysis must be carefully applied since the coherent transfer function of the optical receiver and that due to the L.O.-detector combination are not separable but are related by the convolution of their products. Application of these results to the specific case of a space-lab type optical heterodyne receiver (LHS) shows that resolutions of the order of 1.5-2.0 Km are possible for worst-case type orbital scenarios.

Further, comparison of obscured-type receivers (e.g., Cassegrains) with unobscured receivers shows that both resolution and efficiency are severely degraded in an obscured-type receiver and consequently should not be used for a passive heterodyne detection scheme.

REFERENCES

1. Smith, F. Dow: Optical Image Evaluation and the Transfer Function. Applied Optics, vol. 2, no. 4, April 1963, pp. 335-350.

2. Wolf, William L.; Zissis, George J.; Editors: The Infra-Red Handbook. U.S. Government Printing Office, Washington, D.C., 1978.

3. Goodman, J. W.: Introduction to Fourier Optics. McGraw-Hill, New York, 1968.

4. Yura, H. T.: Optical Heterodyne Signal Power Obtained from Finite Sized Sources of Radiation. Applied Optics, vol. 13, no. 1, Jan. 1974, pp. 150-157.

5. Siegman, A. E.: The Antenna Properties of Optical Heterodyne Receivers. Proc. IEEE, vol. 54, no. 10, Oct. 1966, pp. 1350-1356.

6. Abramowitz, M.; Stegun, I.; Editors: Handbook of Mathematical Functions. National Bureau of Standards Applied Mathematics Series, vol. 55, June 1964, p. 231.

7. Allario, Frank; Katzberg, Stephen J.; Larsen, Jack C.: Sensitivity Studies and Laboratory Measurements for the Laser Heterodyne Spectrometer Experiment. Heterodyne Systems and Technology, NASA CP-2138, 1980. (Paper 17 of this compilation.)
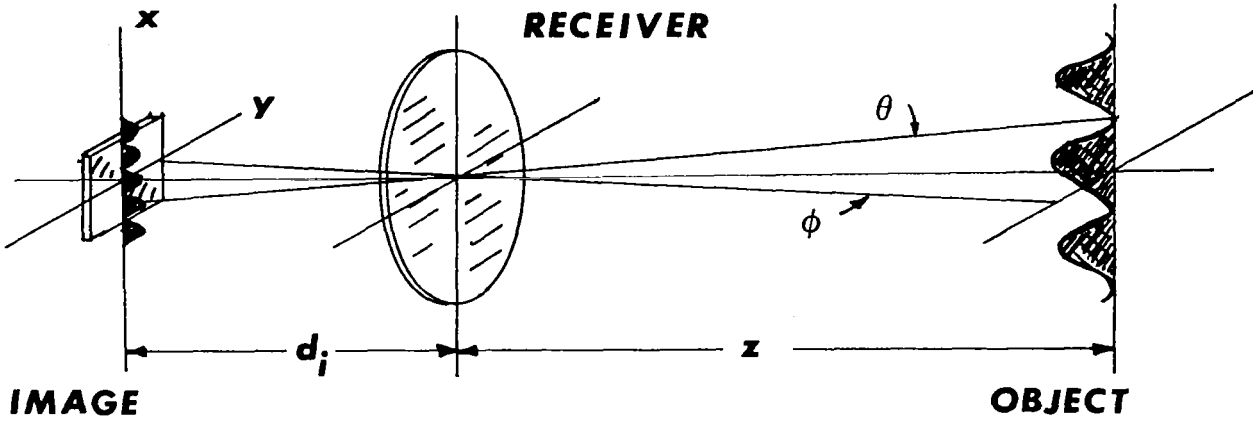
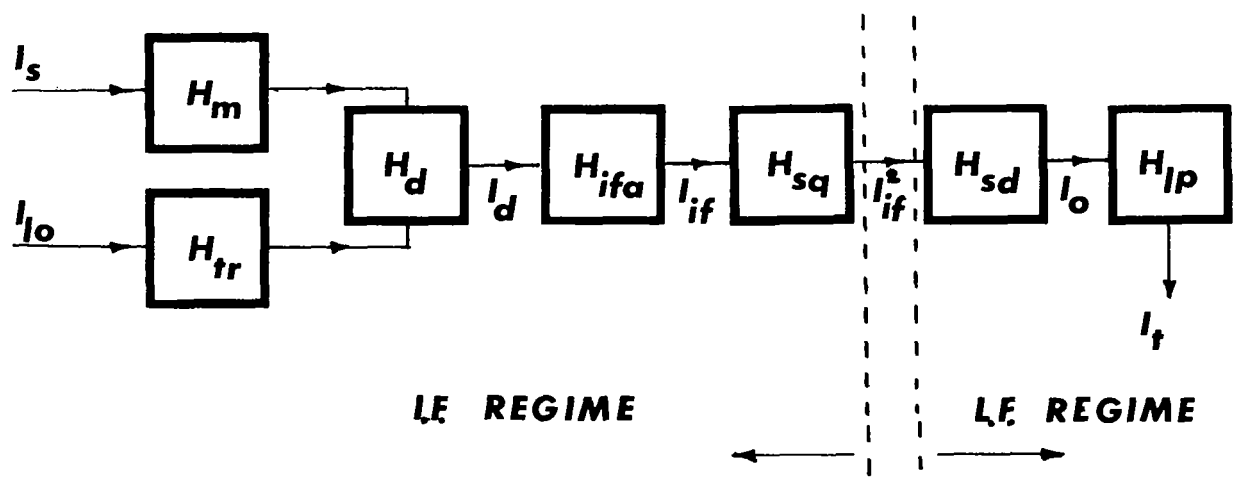Figure 1.- Imaging geometry.

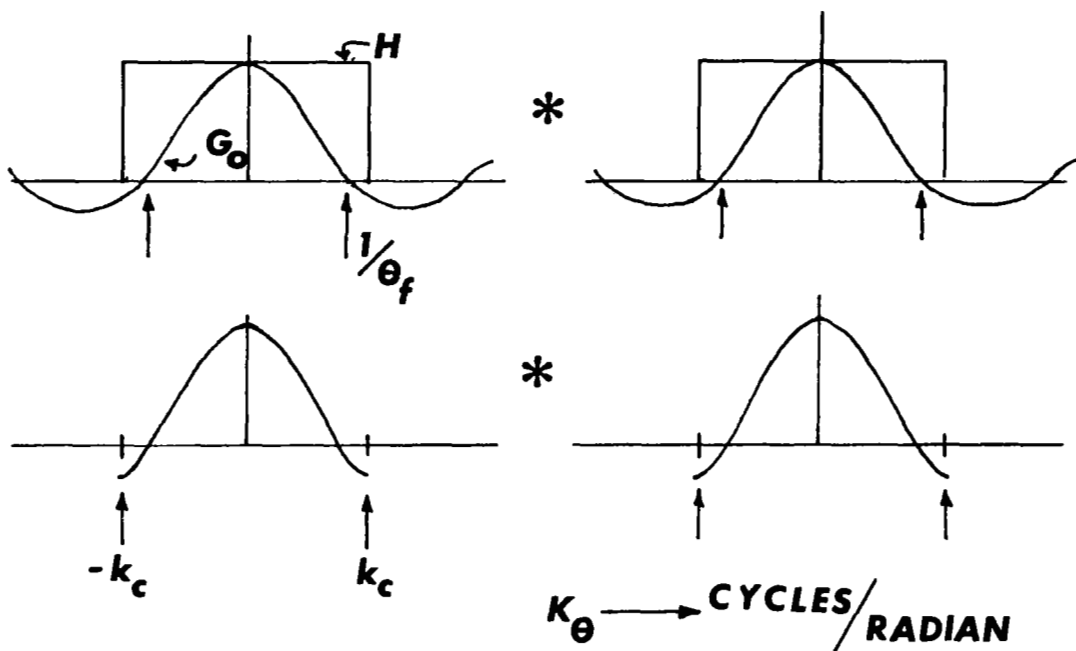Figure 2.- System transfer functions.

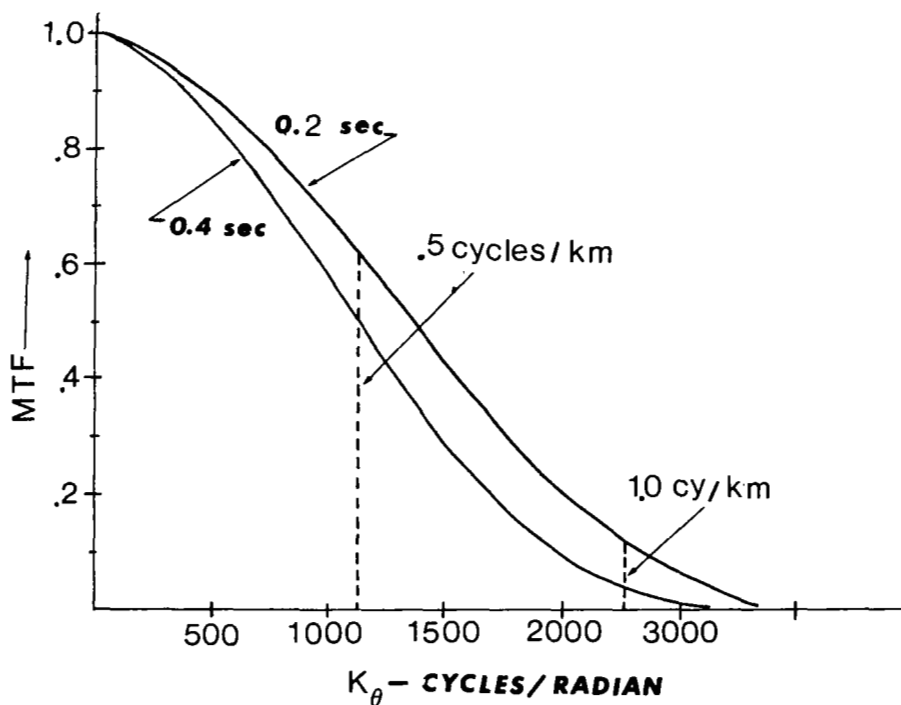Figure 3.- Graphical interpretation of heterodyne transfer function.

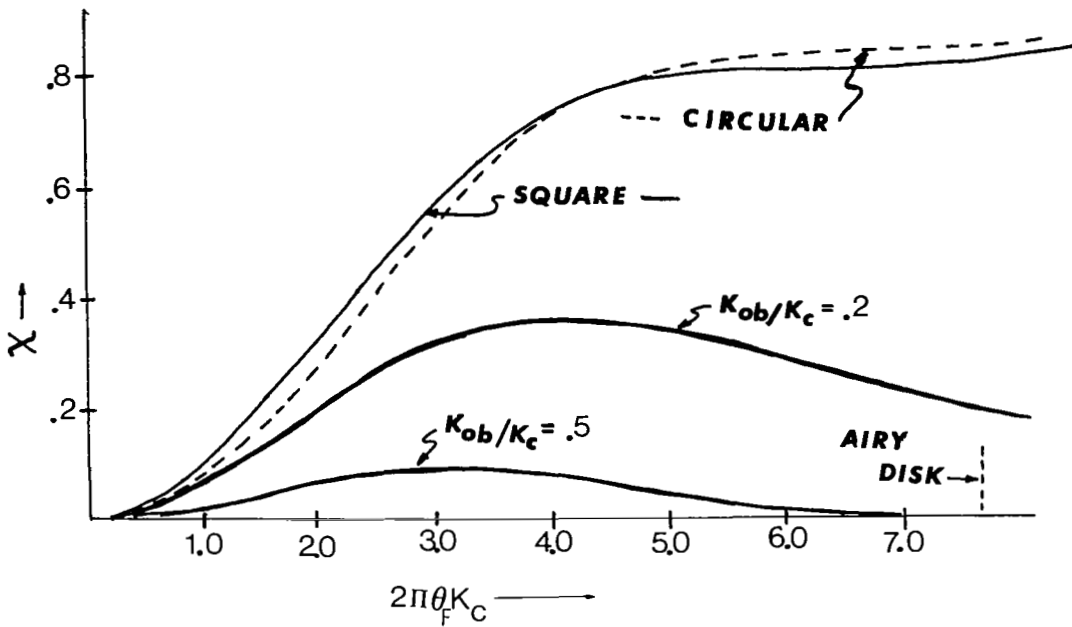Figure 4.- Total MTF for worst-case shuttle orbit and two values of integration time.

Figure 5.- Efficiency factor, χ, versus system parameter $2\pi\theta_F K_C$ for various receiver geometries.
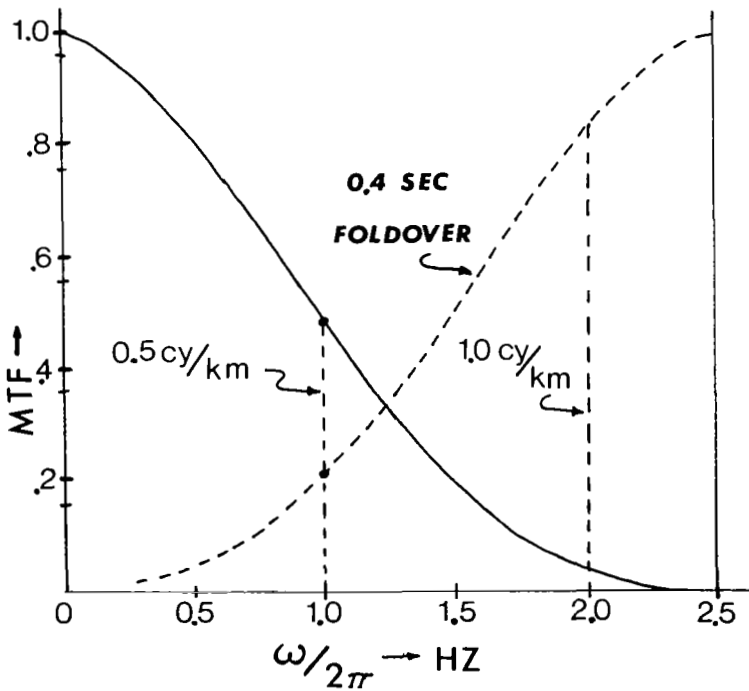

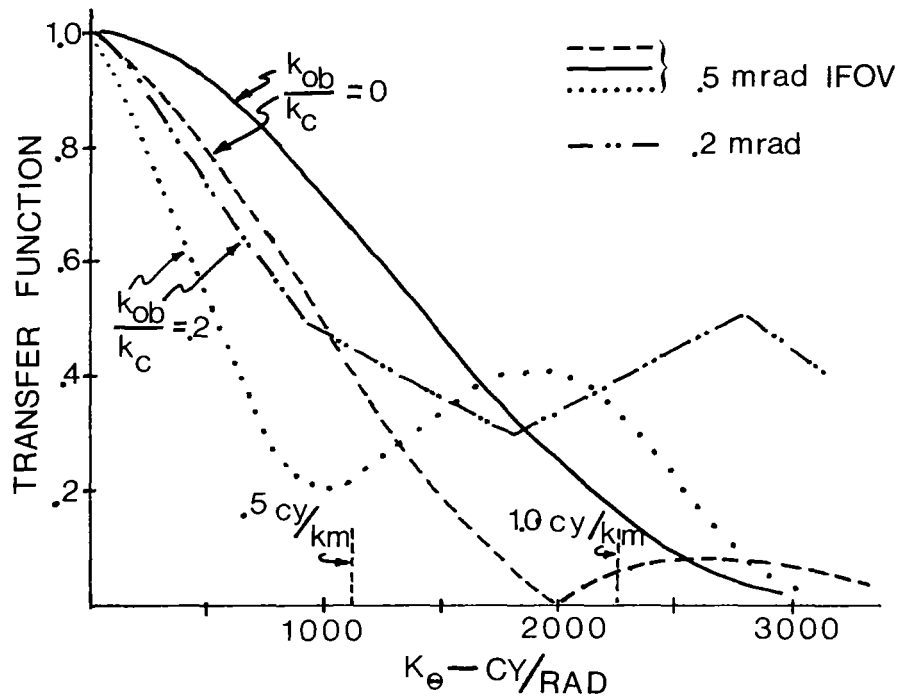Figure 6.- Aliasing error for 2.5 Hz sampling rate at worst-case shuttle orbit.

Figure 7.- Comparison of transfer functions for various geometries. Dashed curve represents conventional MTF with 0.5 mrad I.F.O.V.